Vaccine 37 (2019) 1743–1755

Contents lists available at ScienceDirect

Vaccine

journal homepage: www.elsevier.com/locate/vaccine

Characterization of whole blood transcriptome and early-life fecal microbiota in high and low responder pigs before, and after vaccination for *Mycoplasma hyopneumoniae*

Peris M. Munyaka [a], Arun Kommadath [a,b], Janelle Fouhse [a], Jamie Wilkinson [a,b], Natalie Diether [a], Paul Stothard [a,b], Jordi Estellé [c], Claire Rogel-Gaillard [c], Graham Plastow [a,b], Benjamin P. Willing [a,*]

[a] Department of Agricultural, Food and Nutritional Science, University of Alberta, Canada
[b] Livestock Gentec, University of Alberta, Canada
[c] GABI, INRA, AgroParisTech, Université Paris-Saclay, 78350 Jouy-en-Josas, France

ARTICLE INFO

Article history:
Received 14 September 2018
Received in revised form 1 February 2019
Accepted 11 February 2019
Available online 23 February 2019

Keywords:
Vaccination
Transcriptome
Microbiota
Pig
Prediction
Mycoplasma hyopneumoniae

ABSTRACT

We investigated gene expression patterns in whole blood and fecal microbiota profile as potential predictors of immune response to vaccination, using healthy *M. hyopneumoniae* infection free piglets (n = 120). Eighty piglets received a dose of prophylactic antibiotics during the first two days of life, whereas the remaining 40 did not. Blood samples for RNA-Seq analysis were collected on experimental Day 0 (D0; 28 days of age) just prior to vaccination, D2, and D6 post-vaccination. A booster vaccine was given at D24. Fecal samples for microbial 16SrRNA sequencing were collected at 7 days of age, and at D0 and D35 post-vaccination. Pigs were ranked based on the levels of *M. hyopneumoniae*-specific antibodies in serum samples collected at D35, and groups of 'high' (HR) and 'low' (LR) responder pigs (n = 15 each) were selected. Prophylactic antibiotics did not influence antibody titer levels and differential expression analysis did not reveal differences between HR and LR at any time-point (FDR > 0.05); however, based on functional annotation with Ingenuity Pathway Analysis, D2 post-vaccination, HR pigs were enriched for biological terms relating to increased activation of immune cells. In contrast, the immune activation decreased in HR, 6 days post-vaccination. No significant differences were observed prior to vaccination (D0). Two days post-vaccination, multivariate analysis revealed that *ADAM8*, *PROSER3*, *B4GALNT1*, *MAP7D1*, *SPP1*, *HTRA4*, and *ENO3* genes were the most promising potential biomarkers. At D0, OTUs annotated to *Prevotella*, *CF21*, Bacteroidales and S24-7 were more abundant in HR, whereas *Fibrobacter*, *Paraprevotella*, *Anaerovibrio*, [*Prevotella*], *YRC22*, and *Helicobacter* positively correlated with the antibody titer as well as *MYL1*, *SPP1*, and *ENO3* genes. Our study integrates gene differential expression and gut microbiota to predict vaccine response in pigs. The results indicate that post-vaccination gene-expression and early-life gut microbiota profile could potentially predict vaccine response in pigs, and inform a direction for future research.

1. Introduction

The incidence and severity of infectious diseases has a direct influence on product quality, animal welfare and production economics, hence, animal health and wellbeing are important issues for both producers and consumers. However, strategies aimed at improving animal resistance to specific pathogens may lead to increased susceptibility to other diseases [1]. In order to assess immune capacity or immunocompetence, it is important to understand the molecules that dictate how individuals respond to different stimuli such as infections, vaccination or environmental stresses. Although immune competence is naturally revealed during infection, experimental vaccination addresses many components of the immune system [2]. As such, commercial vaccines, consisting of inactivated, adjuvanted whole-cell preparations, are widely applied worldwide. However, in spite of the fact that the success of vaccination programs is indisputable [3], response to vaccination is highly

Abbreviations: PND, postnatal day; DE, differential expression/differentially expressed; HR, high responder; LR, low responder; OTU, operational taxonomic units; SCFA, short chain fatty acid; TMM, trimmed mean of M-values; CPM, counts per million; IPA, Ingenuity pathway analysis; sPLS, sparse partial least squares; sPLS-DA, sparse least squares discriminant analysis; rCCA, regularized canonical correlation analysis.

* Corresponding author at: Department of Agricultural, Food and Nutritional Science, University of Alberta, Room 310D Ag/For Centre, Edmonton, Alberta T6G 2P5, Canada.
E-mail address: willing@ualberta.ca (B.P. Willing).

https://doi.org/10.1016/j.vaccine.2019.02.016
0264-410X/

variable between individuals, even within apparently homogeneous cohorts [4,5]. In this context, previous studies measuring cell mediated immunity in response to vaccination or immune challenge have indicated a considerable variation among individual pigs [6,7], and serological responses to vaccines have been shown to differ [7]. Therefore, identification of biomarkers that are predictive of a successful vaccine response is of significant importance.

The gut microbiota, which consists of a dynamic community of bacteria, viruses, fungi, and archaea, is known to impact development, maturation and function of the immune system [8–10] and hence, it is a natural extension that the microbiota will impact upon vaccine efficacy. In this context, human and non-human primate studies have suggested a possible link between the microbiota and vaccine efficacy [11–13]. For example, in a model of oral vaccination using heat-labile enterotoxin of enterotoxigenic *Escherichia coli* as adjuvant, depletion of the gut microbiota was associated with depressed Th1 and Th17 responses to the antigen [11], whereas the presence of commensal microbiota in the gut was shown to be crucial for the optimal antibody response to influenza and polio vaccines [13]. Increased gut microbiota community richness and diversity has also been associated with a better response to vaccination [12,14]. The relationship between the host and the composition of gut microbiota is also paramount, considering the influence of both intrinsic and extrinsic factors on the gut microbiota composition [15]. As such, gut microbiota has been shown to suppress serum IgA and IgG responses in conventionally raised mice compared to germ-free mice [10]. In addition, gram-negative gut commensal bacteria have been shown to induce systemic IgG responses under homeostatic conditions, which may contribute to protection against *Escherichia coli* and *Salmonella enterica* infections in both humans and mice [16]. Furthermore, Mach et al. [17] observed that the *Prevotella* enterotype of 70-day-old pigs correlated with higher production of secretory IgA, compared to the *Ruminococcaceae* enterotype, and could be predicted from the abundance of *Clostridium* cluster XIVa and *Lactobacillus* in 14-day-old pigs. This indicates that early-life microbiota is among the factors that program adult microbiota phenotype, and is important for future pig health.

Previous studies investigating transcriptional responses to vaccination in swine have examined transcriptome changes of the peripheral blood mononuclear cells (PBMCs) at different time points following initial and booster vaccinations, and the interactions of the transcriptome changes with lean growth performance [18–20], as well as immune competence following vaccination through antibody measurement and mitogen stimulation [21]. However, the phenotypic variation in host response prior to vaccination that may be associated with variations in vaccine response has not been addressed. In this study we investigated variation in whole blood transcriptome prior to and following vaccination in pigs, using *Mycoplasma hyopneumoniae* vaccine as an exemplifier, and RNA-sequencing technology. In addition, we looked at how the early-life microbiota composition before vaccination may relate to vaccine response, a topic that is majorly unexplored in farm animals. Since *M. hyopneumoniae* is the primary agent involved in porcine enzootic pneumonia, characterized by coughing and decreased performance of the affected pigs [22], the results are of practical relevance to the pig industry.

2. Materials and methods

2.1. Ethical considerations, experimental animals, and antibiotic administration

The experimental protocol was approved by the University of Alberta Animal Care and Use Committee – Livestock, and was conducted at the Swine Research and Technology Centre, University of Alberta, Canada. Animal care, vaccination, injections, and sample collection were performed according to the Canadian Council on Animal Care guidelines. At the time of the experiment, the facility was free of *M. hyopneumoniae* infection and there was no history of vaccinating against it. A total of 120 healthy *M. hyopneumoniae* infection free piglets ((Large White × Landrace) × Duroc) were used in 4 groups of 30 animals to facilitate sample collection and processing. At farrowing, 20 sows (parity ≥ 3) were identified and six piglets closest to the average birth weight of the litter were selected (3 male, 3 female). Of the littermates, four piglets (2 males, 2 females) in the litter received a prophylactic dose of 0.5 mL Oxytetracycline antibiotics at processing (n = 80), whereas the remaining two piglets (1 male, 1 female) did not (n = 40). The antibiotics were introduced to investigate whether this would have any effect on the vaccine response. The piglets were weaned at 21 ± 2 days of age and group housed with their on-trial littermates in nursery pens. Also, body weight was determined at different time-points (at birth, at weaning, and at the end of the experiment (PND 63).

2.2. Vaccination against Mycoplasma hyopneumoniae, fecal and blood sampling

On postnatal day (PND) 28, (Experimental day 0; D0), piglets were vaccinated with RespiSure-ONE (1 mL, intramuscular injection), and a booster vaccine was given at day 24 (D24). Fecal samples for microbiota profiling were collected at 1 week of age (PND 7), prior to vaccination (PND28; D0), and at D35. Blood samples were collected at D0, D2, D6, and D35. The blood samples collected at D0, D2, and D6 were used for gene expression analysis, while the D35 blood samples were used for the quantification of *M. hyopneumoniae*-specific antibodies in serum Fig. 1.

2.3. Sample processing and selection of high (HR) and low (LR) responder pigs

Immediately after collection, fecal samples were placed on ice and later transferred to – 80 °C freezer for storage until use for microbial DNA extraction. Blood samples for gene expression (collected in blue Tempus tubes; ThermoFisher Scientific, Mississauga, ON, CA) were shaken vigorously immediately after collection, placed on ice, and subsequently transferred to – 80 °C freezer, until used for RNA extraction.

Blood samples for humoral immune assay were collected in serum tubes pre-coated with clot activator. Immediately after collection, the tubes were inverted 5–6 times to mix clot activator and allowed to sit for 30 min at room temperature. Next, the samples were centrifuged at 15,000*g* for 10 min at 4 °C, and 1 mL serum was recovered into micro centrifuge tubes, frozen, and shipped to Biovet, Saint-Hyacinthe, QC, Canada for quantification of *M. hyopneumoniae*-specific antibody titers in serum, using the Idexx enzyme-linked immunosorbant assay (ELISA) kit. The anti-*Mycoplasma*-IgG antibody titers varied significantly between vaccinated pigs, with a range of 64-fold difference between the highest and lowest responders. Therefore, for the transcriptome and microbiome analyses, groups of 'high'(HR) and 'low' (LR) responder pigs (n = 15 each) were identified and selected from the extremes of a list of pigs ranked by antibody titers.

2.4. RNA preparation, library construction and Illumina sequencing

Total RNA was extracted from the blood samples collected at D0 and D6 post-vaccination for the HR and LR groups only (n = 15 each), and from all the blood samples collected at D2 (n = 117; 3 pigs were removed from the experiment), using Norgen's Preserved Blood RNA Purification Kit I (Norigen Biotek Corp). The quantity and quality of the RNA were determined using the Agilent

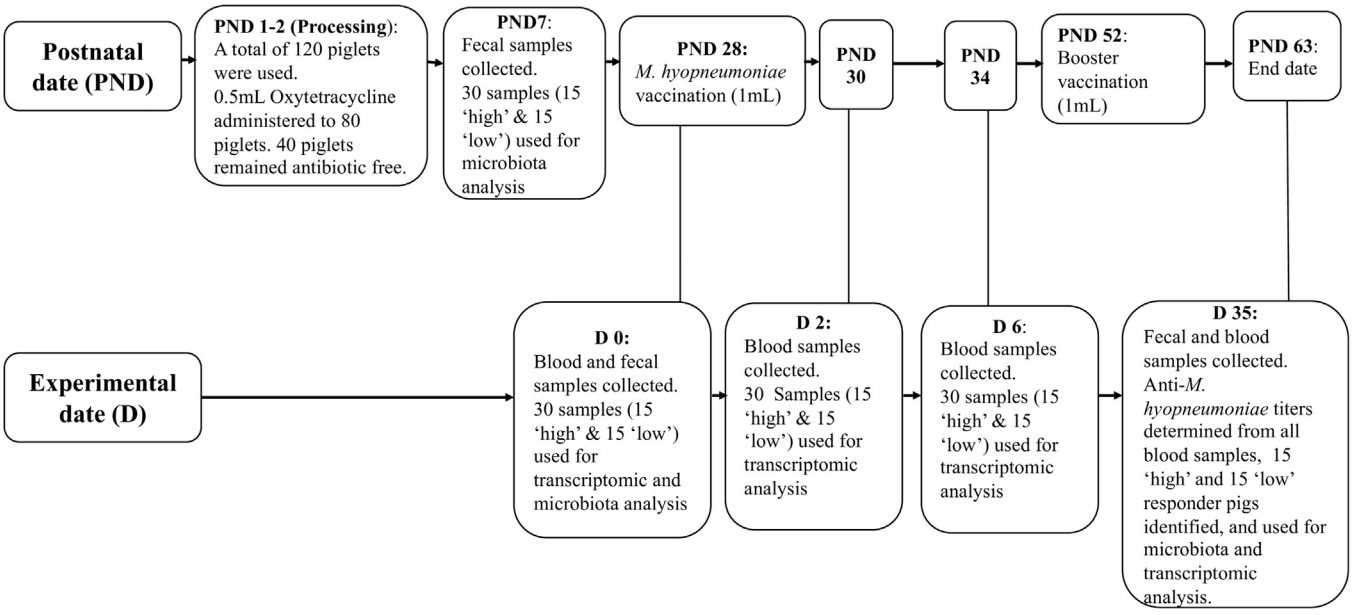

Fig. 1. Experiment groups and study design.

2100 Bioanalyzer (Agilent Technologies, Santa Clara, CA) and Nanodrop 2000 (Thermo Scientific, Wilmington, DE). To enhance the sensitivity of RNAseq to detect differential expression, highly abundant erythrocyte-derived globin transcripts were removed prior to sequencing, as previously described [23]. Next, RNA library was constructed using the Truseq RNA Sample Preparation Kit V2 (Illumina, Inc., San Diego, USA) as described previously [24].

2.5. Identification and quantification of mRNAs

Read processing was conducted as previously described [24]. Briefly, RNA-Seq reads flagged as low quality by the chastity filter in CASAVA 1.8 were removed, as well as reads with an average read quality score below 15 and reads in which over 5 of the last 10 bases had a PHRED quality score below 2. Next, the reads were aligned to pig reference genome sequence assembly (Sscrofa10.2) using Tophat 2.0.12 [25] with default parameters. For annotation of genes, the GTF file for Sscrofa10.2 from Ensembl version 71 was utilized, and the number of reads uniquely mapped to each gene was determined using Htseq-count (v0.6.1) [26]. The Bioconductor (version 3.6) edgeR package (version 3.20.9) was used for further processing of the reads [27] within the R statistical programming language (version 3.4.3). The read counts per gene were normalised to counts per million (CPM). Genes expressed at very low levels were removed by keeping only those genes that achieve CPM above 0.8 in at least fifteen samples, whilst Trimmed mean of M-values (TMM) normalisation was applied to this dataset to account for compositional differences between the libraries. CPM values were used for the differential expression analysis, and clustering of samples by gene expression data (transformed to log2 CPM) was evaluated using multi-dimensional scaling in two dimensions using the *plotMDS* function in the limma (version 3.34.9) package of Bioconductor.

2.6. Differential expression analysis, ingenuity pathway analysis, and multivariate analyses

Differential gene expression between HR and LR responder pigs at each time-point were performed using edgeR. Genes with 1.2-fold change and ordinary P values < 0.05 were uploaded into IPA (IPA; (version 01-12), Ingenuity Systems, Redwood City, CA) to identify relevant categories of molecular pathways, transcriptional networks and biological functions and processes, as derived from the expert annotated database that is provided by the Ingenuity Knowledge Base. The IPA output included biological functions and signalling pathways with statistical assessment of the significance of their representation based on Fisher's Exact test. The biological functions and processes that presented a Z-activation score of 2 and above were considered activated. In addition, 'mixOmics' R package (v 6.3.1) [28–30] was used for the multivariate analysis of the gene expression data, particularly, the sparse Partial Least Squares (sPLS) regression, sparse Partial Least Squares Discriminant Analysis (sPLS-DA), and the regularized canonical correlation analysis (rCCA) [31], in order to identify genes that were more predictive of the observed immune response. sPLS maximises the covariance between two datasets by searching for linear combinations of the variables, and also imposes sparsity within the context of partial least square and thereby carries out dimension reduction and variable selection simultaneously [28,29,31]. The *perf()* function was used to evaluate the model using M-fold cross-validation repeated 60 times. The parameter *Q2.total* was used to tune the number of components using the *perf()* function. The rule of the thumb is that a component should be included in the model if its value is greater than or equal to 0.095. PLS-DA is a supervised approach focusing on the discrimination of the groups being compared [30], whereas sPLS-DA aims to identify a small subset of genes that best discriminate the groups. rCCA identifies and quantifies correlation between two datasets and regularizes the empirical covariance matrices of X and Y by adding a multiple to the identity matrix [31].

2.7. Times series gene expression analysis

Time series expression analysis between HR and LR pigs (across time-points D0, D2, and D6) was conducted using the maSigPro [32] package (version 1.5.0) implemented in R software.

2.8. DNA Extraction, sequencing, bioinformatics and statistical analyses of 16S data

Total DNA was extracted from fecal samples (collected at PND7, D0 and D35 from HR and LR groups only) using a QIAamp stool extraction kit (Qiagen Inc., Valencia, CA), following the protocol for human DNA analysis, and with the addition of a bead-beating step as described

previously [33]. Amplicon libraries from the V3-V4 region of the 16S rRNA gene were constructed and amplified following the Illumina 16S metagenomic sequencing library preparation protocol. The primers targeting this region were: forward, 5′-TCGTCG GCAGCGTCAGATGTGTATAAGAGACAGCCTACGGGNGGCWGCAG-3′; reverse, 5′-GTCTCGTGGGCTCGGAGATGTGTATAAGAGACAGGAC TACHVGGGTATCTAATCC-3′. Paired-end sequencing of the pooled library was performed on an Illumina MiSeq platform (Illumina Inc., San Diego, CA) using 2 × 300 cycles. The raw sequence reads were merged using the PANDAseq algorithm [34], and downstream analysis was performed using QIIME 1.9.1 (Quantitative Insight into Microbial Ecology) software [35]. Briefly, the merged sequences were dereplicated and filtered for chimeras against the Usearch61 algorithms [36], and the sequences retained after the pre-processing steps were used for the open reference-based operational taxonomic units (OTU) picking process, using the green genes database (v. 13.8) clustered at 97% identity.

Species richness estimates (Chao1, Observed OTUs, and abundance-based coverage estimators; ACE), and evenness indices (Shannon and Simpson), were determined at each time-point, using the phyloseq package (v. 1.22.3) implemented in R software (v.3.4.3). Between-sample diversity (beta diversity) was assessed using the unweighted and weighted UniFrac [37] distances and Principal-coordinate analysis (PCoA) was used to visualize these distances using EMPeror [38]. Overall differences between groups in both weighted and unweighted Unifrac distances were compared using Anosim in QIIME.

For microbial characterization, differential abundance at OTU, genus and phylum levels was determined using R package MetagenomeSeq (v 1.20. 1). In this context, low abundant OTUs were filtered to only include OTUs that were present in at least 20% of the samples at each time point, whereas the effect of gender, batch, weaning age, and antibiotics (both HR and LR groups were well represented in the antibiotic groups) were included in the model as cofactors. Next, the list of differentially abundant OTUs between the HR and LR pigs was subjected to multivariate analysis using mixMIC frameworks of the mixOmics (v 6.3.1) R package, and a supervised method sPLS-DA was used to estimate the most contributive OTUs between HR and LR, at each sampling time-point. The OTUs were normalized with a scaling factor method [39]. Additionally, sPLS-DA and Linear discriminant analysis effect size (LEfSe), were used to identify taxa/genera that were more discriminant between the HR and LR groups. For the sPLS-DA analysis, we used the 'mixMC' option in mixOmics R package, whereas for the LEfSe analysis genera that were relatively more abundant in a particular sample group were identified by LEfSe using the Kruskal-Wallis test ($P < 0.05$) and the effect size of each of these genera was estimated using linear discriminant analysis [40]. An LDA score ($\log_{10}$) of 2.0 was used as the cut-off for identifying differentially abundant genera. Finally, sPLS and rCCA were used to highlight correlations between the early-life microbiota and IgG titer measured at D35 or the final body weight, and to integrate the selected OTUs or taxa with the genes that correlated with the levels of *M. hyopneumoniae*-specific IgG at D2 post-vaccination.

Data availability: Raw sequence reads of the 16S rRNA gene amplicon data are available through the SRA with accession number SRP158411.

3. Results

3.1. Administration of prophylactic antibiotics did not influence antibody titers

Based on the ELISA analysis, exposure to prophylactic antibiotics at processing did not influence the *M. hyopneumoniae*-specific antibody titers measured at D35, and hence, the effect of prophylactic antibiotics was either included as a covariate in the subsequent analysis, or not considered at all.

3.2. Blood transcriptome analysis

3.2.1. Biological processes and functions vary between HR and LR groups, D2 post-vaccination

Differential expression analysis by edgeR did not reveal DE genes (FDR > 0.05) between HR and LR at D0, D2, or D6 post-vaccination, and no separation between HR and LR on either day, based on multi-dimensional scaling in two dimensions (data not shown). Also, time series expression analysis by maSigPro did not reveal significant differences between HR and LR across time-points. However, at D2 post-vaccination, IPA showed that the most significantly activated (Z-score ≥ 2) biological functions in HR pigs compared to LR pigs were majorly associated with an increase in biological functions related to migration, recruitment, activation, and adhesion of immune cells (Table 1).

Six days post-vaccination (D6), HR pigs were associated with a decrease in a number of biological functions relating to the activities of various immune cells (Table 2). No significant differences were observed between the HR and LR pigs prior to vaccination (D0).

3.2.2. Discriminant genes between HR and LR pigs and identification of candidate biomarkers

To determine if any of the genes were associated with the HR or LR phenotypes, we performed PLS-DA analysis at D0, D2, and D6 time points. At D0 and D6 time-points, no variables/genes could be selected, suggesting that there were no genes that significantly discriminated between HR and LR groups, and hence, no further analysis could be conducted. At D2 time-point, HR and LR groups were well discriminated, as confirmed by a relatively low performance error rate and the receiver operating characteristic (ROC) curve (Supplementary Fig. 1A–C). The selected genes on the first two components were projected on a loading/contribution plot, a correlation circle, and a cluster image map (Fig. 2 A-C). The genes with the highest contribution in HR pigs include: *ADAM metallopeptidase domain 8* (*ADAM8*), *proline and serine rich 3* (*PROSER3*), *beta-1,4-N-acetyl-galactosaminyltransferase 1* (*B4GALNT1*), and *MAP7 domain containing 1* (*MAP7D1*). Interestingly, rCCA analysis revealed a positive correlation between these genes and the antibody titers. Also, *TAP2*, *MAP7D1* and *ADAM8* showed a positive correlation with the final body weight (Fig. 2 C).

Supplementary data associated with this article can be found, in the online version, at https://doi.org/10.1016/j.vaccine.2019.02.016.

After the sPLS tuning, only three components passed the threshold, and 30 genes that were more predictive of the observed immune response, based on the first two components of the model were identified (Fig. 3 A-B). Interestingly, further rCCA analysis revealed that several genes showed a positive correlation with the antibody titers, including: *SPP1*, *MYL1*, *ENO3*, *HTRA4*, and *PLAU* (Fig. 3 C). Supplementary Fig. 2 shows a graphical visualization of the expression of some of these genes at each time-point.

3.3. Fecal microbiota analysis

3.3.1. Early life microbiota biodiversity and structural changes as a predictor of vaccine response

The phylogenetic diversity measures of the fecal microbiota did not reveal significant differences between HR and LR pigs ($P > 0.05$) at any time-point (data not shown). Similarly, no significant effects were observed on bacterial community composition (beta diversity) on both weighted and unweighted UniFrac distances, except

Table 1
Table listing all the significantly predicted biological processes/functions in HR compared to LR based on the IPA analysis, at D2 post-vaccination. Only those with z-score ≥ 2 are included.

Functions annotation	p-Value	Predicted activation state	Activation z-score	Molecules
Edema	0.0019	Decreased	−2.18	C3,C5AR2,CAV1,F3,F7,KMT2A,MYCN,NCOR1,PLAU,SPHK1
Inflammation of lung	0.0046	Decreased	−2.789	BCL6,C3,CAV1,CBL,CSF2RB,IL2RG,LGALS3,LY96,PLAU,SPHK1
Leukocyte migration	<0.0001	Increased	3.079	ADAM15,ADAM8,ADGRG3,BST1,C3,C5AR2,CAV1,CBL,CHI3L1,CSF2RB,CTGF,F3,F7,GLRX, IL18BP,IL1A,LGALS3,LITAF,LY96,MYB,NPY,PLAU,QPCT,SPHK1, SPP1,THBD
Neovascularization	<0.0001	Increased	2.155	ADAM15,C3,CBL,CTGF,F3,LGALS3,NPY,PLAU,SPHK1,SPP1
Vascularization	<0.0001	Increased	2.355	ADAM15,B4GALNT1,C3,CBL,CTGF,F3,LGALS3,NPY,PLAU,SPHK1,SPP1
Proliferation of lymphatic system cells	<0.0001	Increased	2.91	BCL6,C3,CAV1,CBL,CHI3L1,CSF2RB,CTGF,FTL,GAPT,IL1A,IL2RG,KMT2A,LGALS3,LY96, MYB,MYCN,NPY,PLAU,RELT,SOX13,SPP1,VSIG4
Adhesion of vascular endothelial cells	<0.0001	Increased	2.575	ADAM15,F3,IL1A,LGALS3,LGALS8,NPY,SPP1
Development of vasculature	<0.0001	Increased	2.208	ADAM15,ADAM8,BMP1,C3,CAV1,CBL,CHI3L1,CSF2RB,CTGF,F3,F7, GLRX,IL18BP,IL1A,KMT2A,LGALS3,LGALS8,MYB,MYCN,NPY,PLAU,SMAD9,SPHK1, SPP1,THBD, ZMYND10
Proliferation of lymphocytes	<0.0001	Increased	2.492	BCL6,C3,CAV1,CBL,CSF2RB,CTGF,FTL,GAPT,IL1A,IL2RG,LGALS3,LY96,MYB,MYCN, NPY,PLAU,RELT,SOX13,SPP1,VSIG4
Cell movement of granulocytes	<0.0001	Increased	2.065	ADAM15,ADAM8,BST1,C3,C5AR2,CTGF,F3,IL1A,LGALS3,PLAU,SPHK1,SPP1, THBD
Engulfment of granulocytes	<0.0001	Increased	2	C3,CSF2RB,GLRX,IL1A,PLAU
Quantity of connective tissue	0.0001	Increased	3.223	B4GALNT1,C3,CAV1,CBL,CTGF,GPAT3,IL1A,MYB,NBEAL2,NCOR1,NPY, PICALM, PILRA,PLAU,PSTPIP2,SPHK1,SPP1
Adhesion of immune cells	0.0001	Increased	2.496	C3,C5AR2,CSF2RB,F3,GLRX,IL1A,LGALS3,NPY,PILRA,PLAU,SPP1,THBD
Cell movement of myeloid cells	0.0001	Increased	2.261	ADAM15,ADAM8,BST1,C3,C5AR2,CAV1,CTGF,F3,IL1A,LGALS3, LITAF,PLAU, QPCT, SPHK1,SPP1,THBD
Cell movement of leukocytes	0.0001	Increased	2.57	ADAM15,ADAM8,BST1,C3,C5AR2,CAV1,CTGF,F3,F7,IL18BP,IL1A, LGALS3, LITAF,MYB,NPY,PLAU,QPCT,SPHK1,SPP1,THBD
Cell movement of phagocytes	0.0001	Increased	2.249	ADAM15,ADAM8,BST1,C3,C5AR2,CAV1,CTGF,IL1A,LGALS3,LITAF,NPY,PLAU,QPCT, SPHK1,SPP1,THBD
Proliferation of blood cells	0.0001	Increased	2.848	BCL6,C3,CAV1,CBL,CSF2RB,CTGF,FTL,GAPT,IL1A,IL2RG,KMT2A,LGALS3, LY96,MYB,MYCN,NPY,PLAU,RELT,SOX13,SPP1,VSIG4
Recruitment of granulocytes	0.0001	Increased	2.804	C3,CAV1,CHI3L1,CSF2RB,GLRX,IL1A,LGALS3,LY96,SPP1
Angiogenesis	0.0001	Increased	2.208	ADAM15,ADAM8,C3,CAV1,CBL,CHI3L1,CSF2RB,CTGF,F3,GLRX,IL18BP,IL1A,KMT2A,LGALS3,LGALS8,MYB, NPY,PLAU,SPHK1,SPP1,THBD,ZMYND10
Binding of blood cells	0.0002	Increased	2.687	C3,C5AR2,CSF2RB,F3,GLRX,IL1A,LGALS3,NPY,PILRA,PLAU,SIGLEC5,SPP1, THBD
Binding of fibroblast cell lines	0.0002	Increased	2.144	CBL,CTGF,IL2RG,LGALS8,SIGLEC5,SPP1
Recruitment of myeloid cells	0.0002	Increased	2.959	C3,CAV1,CHI3L1,CSF2RB,F3,GLRX,IL1A,LGALS3,LY96,SPP1
Cell proliferation of T lymphocytes	0.0002	Increased	2.054	C3,CAV1,CBL,CSF2RB,CTGF,FTL,IL1A,IL2RG,LGALS3,MYB,NPY,PLAU, RELT,SOX13, SPP1,VSIG4
Activation of cells	0.0002	Increased	3.216	ADAM8,C3,CBL,CHI3L1,CSF2RB,CTGF,F3,F7,ICA1,IL1A,IL2RG,KLRF1, LGALS3,LY96, MYCN,NBEAL2,NPY,PLAU,SIRPG,SPP1,TAS1R3,THBD
Activation of blood cells	0.0002	Increased	2.718	C3,CBL,CHI3L1,CSF2RB,F3,F7,ICA1,IL1A,IL2RG,KLRF1,LGALS3,LY96,MYCN,NBEAL2,NPY,SIRPG,SPP1,THBD
Cell movement of antigen presenting cells	0.0004	Increased	2.051	C3,CAV1,CTGF,IL1A,LGALS3,LITAF,NPY,PLAU,SPHK1,SPP1,THBD
Cell movement	0.0006	Increased	3.586	ADAM15,ADAM8,ADGRG3,BST1,C3,C5AR2,CAV1,CBL,CDH4,CHI3L1,CSF2RB,CTGF,DNAH1,F3,F7,FNDC3B,GLRX,IL18BP,IL1A,KMT2A,LGALS3,LGALS8, LITAF,LY96,MAP3K12,MBOAT7,MYB,NPY,P4HA2,PLAU,QPCT, SH3BP1, SPHK1,SPP1,TAS1R3,THBD,TP53INP2,ZMYND10
Inflammatory response	0.0007	Increased	2.416	ADAM8,BCL6,BST1,C3,C5AR2,CAV1,CHI3L1,F7,IL1A,LGALS3,LITAF,LY96, mir-147,NPY,PLAU,SPHK1,SPP1,THBD
Recruitment of leukocytes	0.0007	Increased	2.964	C3,CAV1,CHI3L1,CSF2RB,F3,GLRX,IL1A,LGALS3,LY96,SPP1
Migration of phagocytes	0.0007	Increased	2.94	ADAM15,BST1,C3,CTGF,LGALS3,NPY,PLAU,QPCT,SPP1
Phagocytosis of cells	0.0009	Increased	2.174	C3,CAV1,CBL,CSF2RB,GLRX,LGALS3,NPY,PEAR1,PLAU
Internalization of cells	0.0009	Increased	2.371	C3,CBL,CSF2RB,GLRX,LGALS3,LY96,PEAR1,PLAU
Recruitment of neutrophils	0.0009	Increased	2.433	CAV1,CHI3L1,GLRX,IL1A,LGALS3,LY96,SPP1
Migration of cells	0.0010	Increased	3.314	ADAM15,ADAM8,ADGRG3,BST1,C3,C5AR2,CAV1,CBL,CHI3L1,CSF2RB,CTGF,F3,F7,FNDC3B,GLRX,IL18BP,IL1A,KMT2A,LGALS3,LITAF,LY96,MAP3K12, MBOAT7,MYB,NPY,P4HA2,PLAU,QPCT,SH3BP1,SPHK1,SPP1,THBD,TP53INP2,ZMYND10
Adhesion of phagocytes	0.0012	Increased	2.168	C3,F3,GLRX,IL1A,NPY,PLAU
Migration of granulocytes	0.0012	Increased	2.401	ADAM15,BST1,C3,F3,PLAU,SPP1
Vasculogenesis	0.0014	Increased	2.139	ADAM15,C3,CAV1,CBL,CSF2RB,CTGF,F3,GLRX,IL18BP,IL1A,KMT2A, LGALS3,NPY,PLAU, SPHK1,SPP1,THBD

(*continued on next page*)

Table 1 (*continued*)

Functions annotation	p-Value	Predicted activation state	Activation z-score	Molecules
Activation of endothelial cells	0.0015	Increased	2	C3,F3,IL1A,PLAU
Cell movement of endothelial cells	0.0016	Increased	2.324	ADAM15,ADGRG3,CAV1,CTGF,F3,KMT2A,LGALS3,PLAU,SPP1,THBD
Recruitment of phagocytes	0.0016	Increased	2.621	CAV1,CHI3L1,F3,GLRX,IL1A,LGALS3,LY96,SPP1
Concentration of phosphatidic acid	0.0017	Increased	2.195	CAV1,F7,IL1A,LGALS8,MBOAT7,SPP1
Engulfment of cells	0.0020	Increased	2.324	C3,CAV1,CBL,CSF2RB,GLRX,IL1A,LGALS3,NPY,PEAR1,PICALM, PLAU
Uptake of D-glucose	0.0024	Increased	2.02	CAV1,CBL,CPT1C,MEDAG,NPY,PLAU,SPP1
Uptake of monosaccharide	0.0024	Increased	2.02	C3,CAV1,CBL,CPT1C,MEDAG,NPY,PLAU,SPP1
Transmigration of cells	0.0025	Increased	2.425	ADAM15,BST1,CAV1,F3,NPY,SPP1
Proliferation of hematopoietic cells	0.0028	Increased	2.562	CBL,CSF2RB,IL1A,IL2RG,KMT2A,LGALS3,MYB,SPP1
Migration of endothelial cells	0.0030	Increased	2.524	ADAM15,ADGRG3,CAV1,CTGF,F3,KMT2A,PLAU,SPP1,THBD
Cell spreading	0.0033	Increased	2.053	BST1,C3,CBL,LGALS3,LGALS8,PLAU,SPHK1,SPP1
Engulfment of leukocytes	0.0039	Increased	2.148	C3,CSF2RB,GLRX,IL1A,LGALS3,PLAU
Endotoxin shock response	0.0041	Increased	2	CAV1,F3,LY96,SPHK1
Cell movement of connective tissue cells	0.0042	Increased	2.384	CAV1,CBL,CTGF,F7,FNDC3B,PLAU,SPP1
Migration of connective tissue cells	0.0047	Increased	2.18	CAV1,CBL,CTGF,FNDC3B,PLAU,SPP1
Activation of leukocytes	0.0058	Increased	2.672	C3,CBL,CHI3L1,CSF2RB,F7,ICA1,IL1A,IL2RG,KLRF1,LGALS3,LY96, NPY,SIRPG,SPP1

at D0 time-point where the weighted Unifrac distance differed between HR and LR ($P = 0.0429$), suggesting an effect of more abundant bacteria (data not shown). At PND7 time-point, only 24 OTUs were found to be differentially abundant between the HR and LR pigs, and sPLS-DA analysis of these OTUs showed that OTUs annotated to Lachnospiraceae, *Parabacteroides distansosis*, *Bacteroides ovatus, Bacteroides* and *Sphaerochaeta* best discriminated the HR compared to LR group (Fig. 4 A). Also, sPLS-DA analysis revealed that genera *Actinomyces, Clostridium, Peptostreptococcus*, *Butyricimonas*, *Roseburia*, *Coprococcus*, *Prevotella* unclassified Lachinospiraceae, among others discriminated the HR group from the LR group (Fig. 4 B). Based on the LEfSe analysis, genera *Arcanobacterium* unclassified Actinomycetaceae, and unclassified Actinobacteria were enriched in the HR compared to LR group (Fig. 4C). Correlation analysis at genus level revealed that *Butyricimonas*, *Roseburia* and *CF231* genera positively correlated with the antibody titers, and a similar pattern of correlation with the final body weight was observed (Fig. 4 D). At D0 time-point, a total of 67 OTUs were differentially abundant between HR and LR pigs. In this context, most of the OTUs annotated to *Prevotella*, CF21, Bacteroidales and S24-7 were more abundant in HR pigs compared to the LR pigs (Fig. 5 A), and correlation analysis revealed their positive association with the antibody titer, and with *MYL1*, *SPP1*, and *ENO3* genes (Fig. 5 B, C). At the genus level, *Fibrobacter*, *Sharpea*, *Paraprevotella*, *Anaerovibrio*, [*Prevotella*], *YRC22*, *pyramidobacter*, and *Helicobacter* positively correlated with the antibody titer, and some of these genera also had a positive correlation with *SPP1*, *MYL1*, *ENO3*, *SLN*, and *PDPN* genes (Fig. 5 D, E). At D35, a total of 39 OTUs were differentially abundant between HR and LR pigs, with several OTUs annotated to *Succinivibrio*, and S24-7 being more abundant in HR compared to LR (data not shown). Correlation analysis did not reveal any positive association between the OTUs and the antibody titers.

4. Discussion

The evidence of genetic variation and several breeding approaches to improve the genetic potential for immunocompetence has been pointed out and discussed in the past [41]. Our aim was to profile whole blood transcriptome in HR and LR pigs in order to identify genes whose expression correlate with specific antibody titer levels to predict vaccine response prior to vaccination, using *M. hyopneumoniae* vaccination. Initial microarray characterization of transcriptional *in vivo* response of porcine PBMCs to immune stimulation using tetanus toxoid as a model antigen [19] revealed considerable changes on the mRNA levels very early after vaccination, and a decrease in the number of DE genes at a later date post-vaccination. The study also reported an earlier broad transcriptional response of naïve PBMCs following vaccination, whereas Regnstrom and colleagues [42] observed an immediate transcriptional response of murine spleen cells, 4 h after *in vitro* stimulation by tetanus toxoid. Also, studies looking at transcriptome changes following experimental *Salmonella* infection in pigs have reported substantial whole blood transcriptome changes 2 days post-infection compared to day 0 in both low and persistent shedders, but not before infection [24,43]. Although our study took a different approach, these studies agree with the fact that we were also unable to detect DE genes between HR and LR pigs prior to vaccination, and even after vaccination. This could be due to the relatively small sample size and variability among samples within each group that reduce the power to detect changes in expression, coupled with the strict multiple testing corrections, or due to factors relating to the vaccine itself that may make it difficult to detect differentially expressed genes. Hence, a broader or more sensitive approach may be required in order to identify those

Table 2
Table listing all the significantly predicted biological processes/functions in HR compared to LR based on the IPA analysis, at D6 post-vaccination. Only those with z-score $\geq$ 1.5 are included.

Functions annotation	p-Value	Predicted activation state	Activation z-score	Molecules
Cell movement	0.0001	Decreased	−2.748	AGER,APBB2,C3AR1,CADPS2,CD34,CEBPB,CSF2RA,IFT88,KCNN3, LAMB1,LTF,MMP8,MSR1,NCAM1,NLRP3,NRG1,PGLYRP1,PRKAA1, SCLT1, SNCG,SPARCL1,SPP1,STK3,THBD,TNFAIP6,TNFRSF10A
Migration of cells	0.0001	Decreased	−2.684	AGER,APBB2,C3AR1,CADPS2,CD34,CEBPB,CSF2RA,KCNN3,LAMB1, LTF,MMP8,MSR1,NCAM1,NLRP3,NRG1,PGLYRP1,PRKAA1,SNCG, SPARCL1, SPP1,STK3,THBD,TNFAIP6,TNFRSF10A
Quantity of cells	0.0005	Decreased	−2.557	AGER,C3AR1,CADPS2,CD34,CEBPB,CYP27B1,IFT88,MMP8,MPL, MSR1,NCAM1,NLRP3,NRG1,PGLYRP1,PRKAA1,SNCG,SPP1,STK3, THBD,TNFAIP6, TNFRSF10A
Differentiation of connective tissue cells	0.0021	Decreased	−2.377	AGER,C3AR1,CEBPB,IFT88,LTF,MEDAG,NLRP3,NRG1,SPP1,STK3
Proliferation of muscle cells	0.0026	Decreased	−2.377	AGER,C3AR1,MMP8,NRG1,SPP1,THBD,TNFRSF10A
Activation of antigen presenting cells	0.0040	Decreased	−2.236	AGER,CEBPB,LTF,MSR1,NRG1,TNFRSF10A
Quantity of blood cells	0.0032	Decreased	−2.214	AGER,C3AR1,CD34,CEBPB,CYP27B1,MMP8,MPL,NLRP3,PGLYRP1, PRKAA1,SPP1,THBD,TNFRSF10A
Inflammatory response	0.0001	Decreased	−2.201	AGER,C3AR1,CEBPB,CSF2RA,HPGDS,LTF,MMP8,MSR1,NLRP3,NRG1,PGLYRP1,SPP1,THBD,TNFAIP6
Proliferation of smooth muscle cells	0.0021	Decreased	−2.178	AGER,C3AR1,MMP8,SPP1,THBD,TNFRSF10A
Proliferation of immune cells	0.0071	Decreased	−2.145	AGER,CEBPB,CSF2RA,DNTT,HPGDS,LTF,MPL,NRG1,SPP1,TNFRSF10A
Delayed hypersensitive reaction	0.0002	Decreased	−2	AGER,CEBPB,NLRP3,SPP1,THBD
Quantity of myeloid cells	0.0029		−1.981	AGER,C3AR1,CD34,MMP8,MPL,PGLYRP1,SPP1,THBD
Metabolism of eicosanoid	0.0001		−1.967	AGER,CEBPB,CYP2C18,HPGDS,LTF,NCAM1,NRG1
Immune response of T lymphocytes	0.0023		−1.949	AGER,C3AR1,HPGDS,MSR1
Activation of phagocytes	0.0021		−1.912	AGER,CEBPB,LTF,MSR1,NRG1,SPP1,TNFRSF10A
Uptake of D-glucose	0.0005		−1.775	CEBPB,IFT88,MEDAG,NRG1,PRKAA1,SPP1
Vasculogenesis	0.0073		−1.768	AGER,C3AR1,CD34,FBLN1,IFT88,NRG1,PRKAA1,SPP1,STK3,THBD
Phagocytosis	0.0040		−1.747	AGER,C3AR1,CEBPB,EPG5,MSR1,PGLYRP1
Proliferation of blood cells	0.0055		−1.72	AGER,CD34,CEBPB,CSF2RA,DNTT,HPGDS,LTF,MPL,NRG1,SPP1, TNFRSF10A
Activation of myeloid cells	0.0059		−1.664	AGER,CEBPB,LTF,MSR1,NRG1,SPP1
Immune response of leukocytes	0.0001		−1.571	AGER,C3AR1,CEBPB,HPGDS,MSR1,PGLYRP1,PRKAA1,THBD

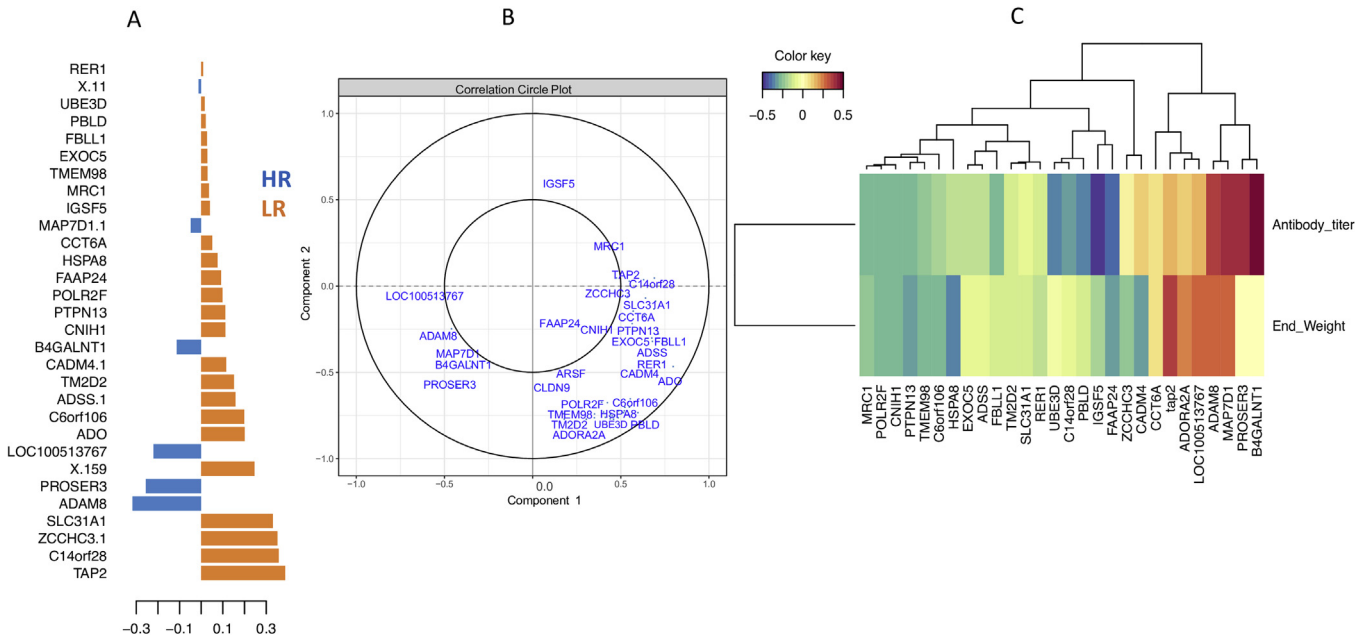

Fig. 2. A–C: Supervised analysis and feature selection with sPLS-DA at D2 time-point. A; Loading plot of each feature selected on the first component, with color indicating the group with a maximal mean expression value for each gene, B; Correlation circle plot representing each type of selected features, C; Clustered Image Map (Euclidean Distance, Complete linkage) showing the correlation between the antibody titer and final body weight with sPLS-DA-selected genes. Antibody titer and final body weight are represented in rows, selected features on the first component in columns with deep brown showing positive correlation and deep blue a negative correlation.

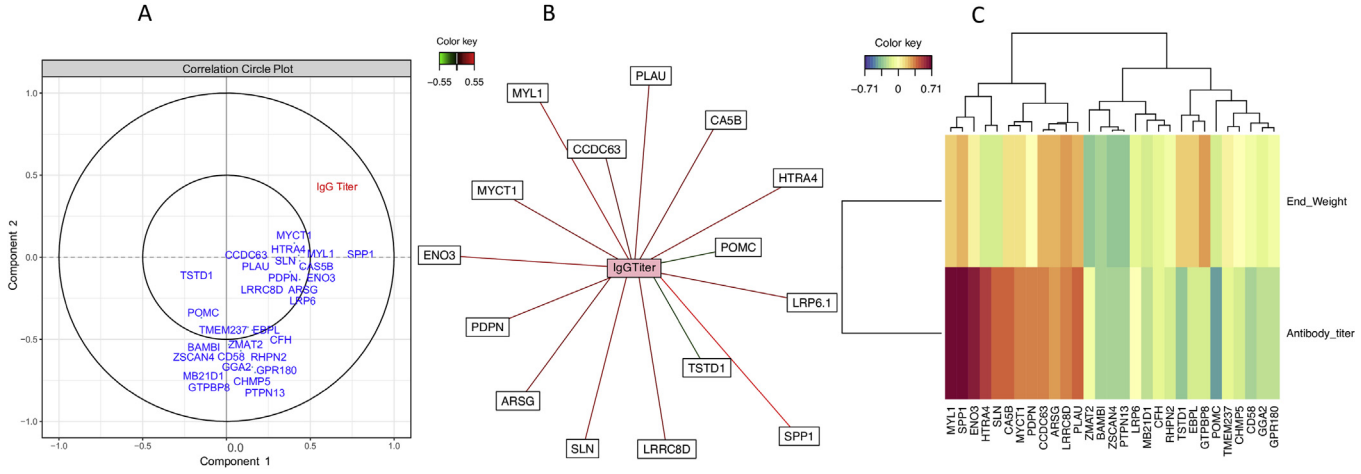

Fig. 3. A-C: Unsupervised analysis and feature selection with sparse PLS at D2. A; Correlation Circle plots for the first two sPLS dimensions (30 genes selected in total). The circle displays the antibody titer (IgGTiter) and the selected genes. The nature of the correlation between two variables can be visualised through the angles between two vectors: a sharp angle indicates positive correlation, an obtuse angle indicates negative correlation, and a right angle indicates no correlation, B; Relevance network highlighting the association between the IgGTiter and selected genes. Red and green edges indicate positive and negative correlation, respectively, C; Clustered Image Map showing the correlation between the antibody titer and final body weight with sPLS-DA-selected genes. Antibody titer and final body weight are represented in rows, selected features on the first component in columns with deep brown showing a positive correlation and deep blue a negative correlation.

genes. Therefore, we employed alternative approaches including IPA and empirical multivariate analysis in order to find potential putative predictors of vaccine response.

Comparison of D0 transcriptome profiles performed among the HR and LR groups using IPA did not reveal significant differences in terms of affected canonical pathways or biological functions. This indicates that the animals were in a naïve state before the vaccination, or that the experiment did not have sufficient power to detect differences at baseline due to similar reasons cited above. Nevertheless, at two days post-vaccination, the HR group had a general increase in predicted biological functions related to increased activation of immune cell activities, compared to LR transcripts. However, six days post-vaccination, HR pigs were associated with a significant decrease in the biological processes associated with activation of immune cell activities. On the one hand, this may suggest that HR pigs had more immunologically competent cells prior to vaccination, and were more able to mount an immune response following vaccination, and that possibly tissue reorganization and cell population modifications occurred by 6 days post-vaccination, consequently reducing the immune activities. On the other hand, the results suggest presence of less competent immune cells in LR pigs, as while the HR responded quickly and were able to

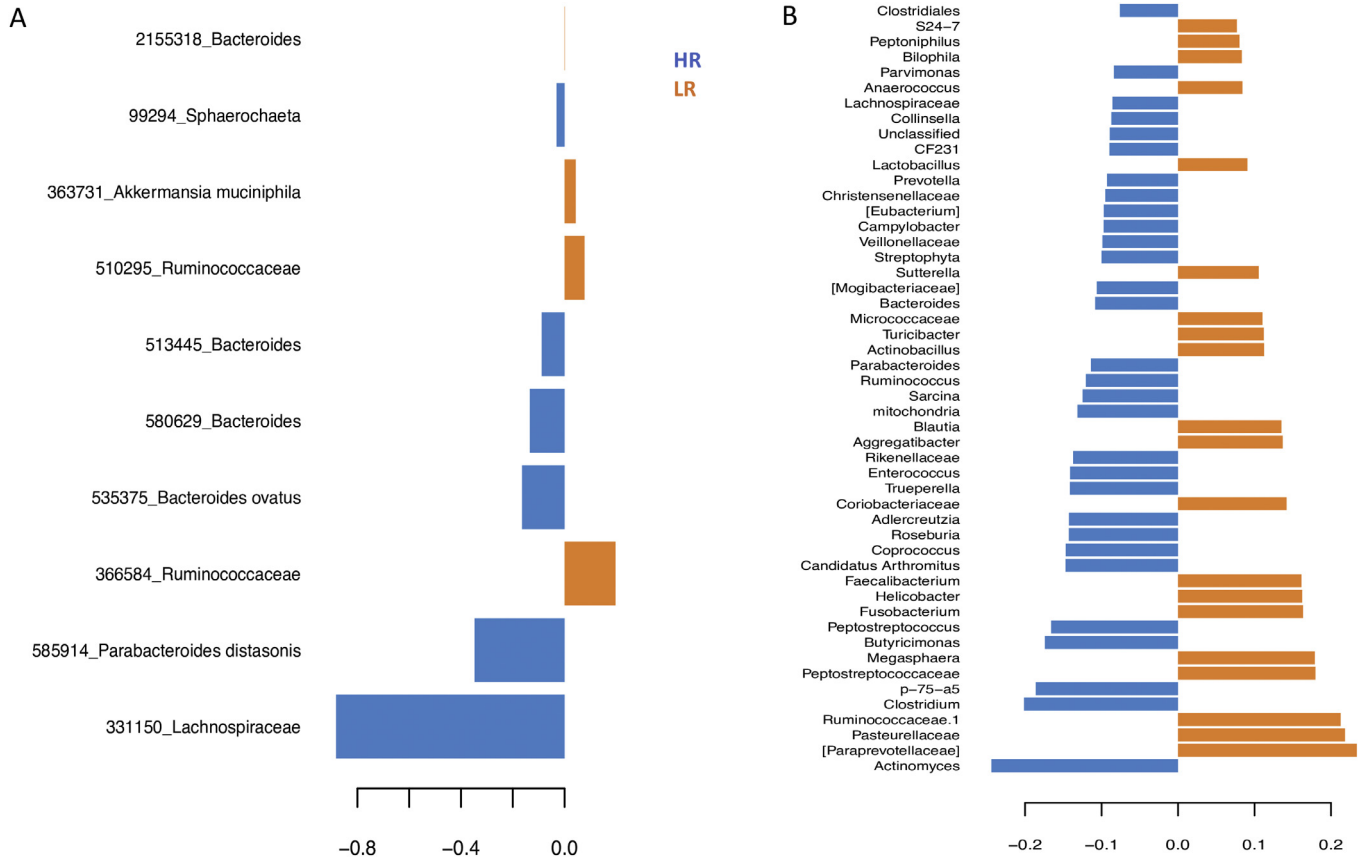

Fig. 4A-B. Analysis of the differentially abundant or discriminant genus or OTUs in HR and LR pigs, at PND 7. A; Loading plot of each OTU selected on the first component, with color indicating the group with a maximal mean expression value for each OTU. Differential abundance between the HR and LR was analyzed using MetagenomeSeq and the differentially abundant OTUs (27) were subjected to sPLS-DA analysis, B; Loading plot of each genera selected on the first component, with color indicating the group with a maximal mean expression value for each genera as analyzed using sPLS-DA.

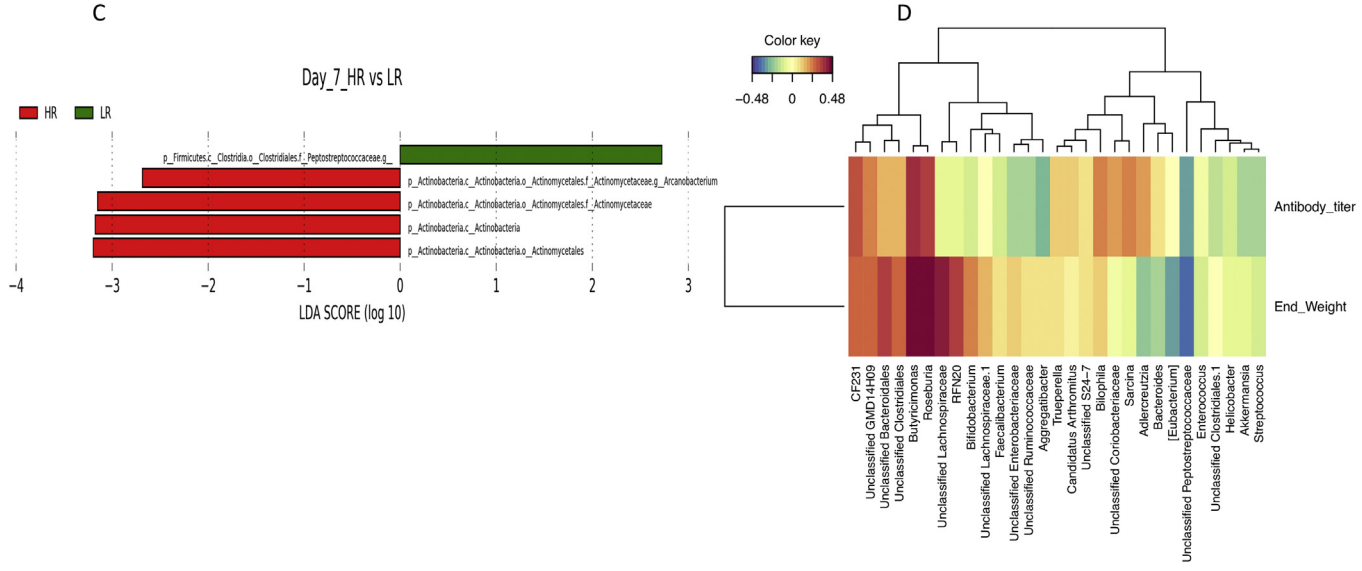

Fig. 4C-D. Discriminant genera or OTUs in HR and LR pigs, and correlation analysis between the discriminant taxa/OTUs and the antibody titer or the final body weight, at PND 7. C; Discriminant taxa as analyzed using Linear Discriminant Analysis with Effect size (LeFSe), D; Clustered Image Map (Euclidean Distance) showing the correlation between the antibody titer and final body weight with taxa at genus level.

return back to normal by 6 days, the LR had a delayed response. These findings are in agreement with previous studies that reported increased transcripts related to immune responses and other biological functions within the first 24 h following vaccination and more decreased transcripts several days (14) after the initial vaccination [18,20]. *Secreted phosphoprotein 1*, (*SPP1*),

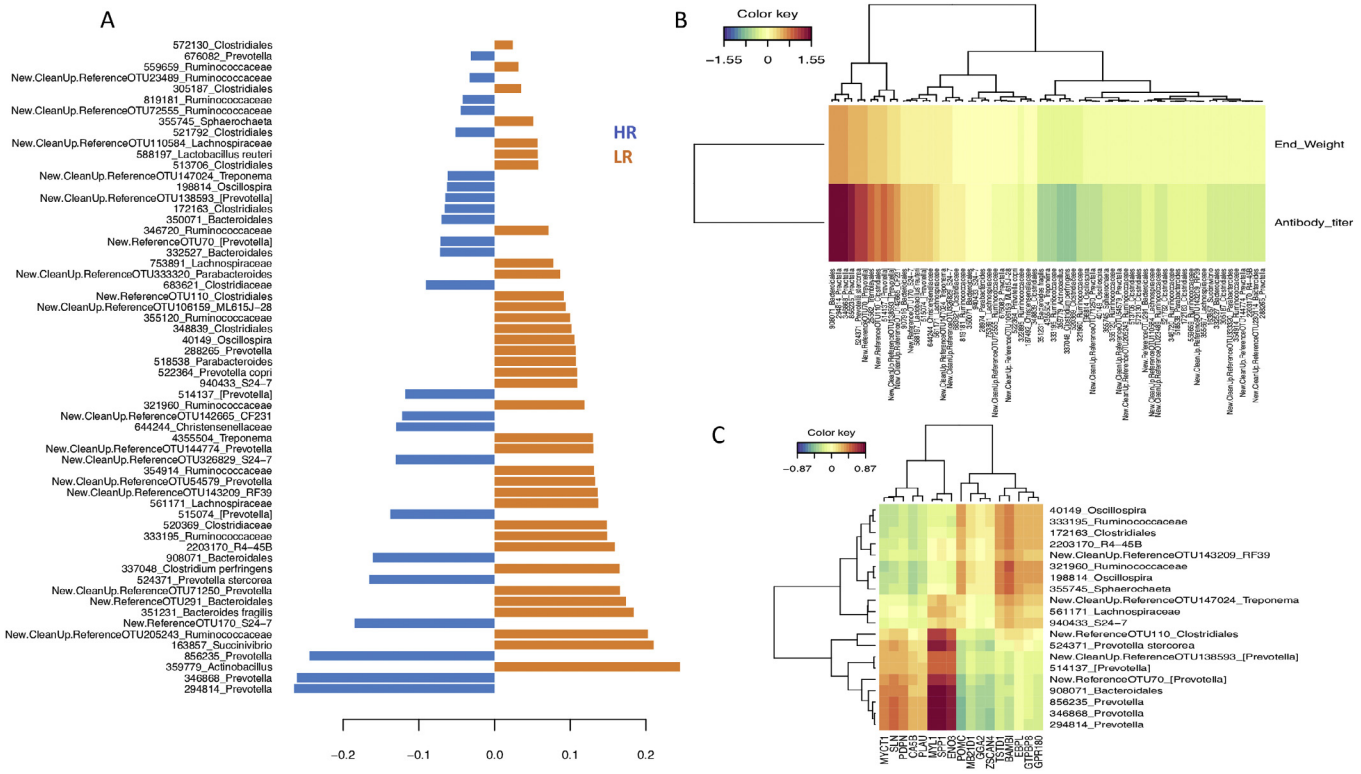

Fig. 5A-C. Analysis of the differentially abundant or discriminant OTUs in HR and LR pigs, and correlation analysis between the discriminant OTUs and the antibody titer or the final body weight, or with the selected genes, at D0 time-point. A; Loading plot of each OTU selected on the first component, with color indicating the group with a maximal mean expression value for each OTU. Differential abundance between the HR and LR was analyzed using MetagenomeSeq and the differentially abundant OTUs (67) were subjected to sPLS-DA analysis, B; Clustered Image Map (Euclidean Distance) showing the correlation between the antibody titer and final body weight with the differentially abundant OTUs, C; Clustered Image Map showing the correlation between the selected genes with the differentially abundant OTUs.

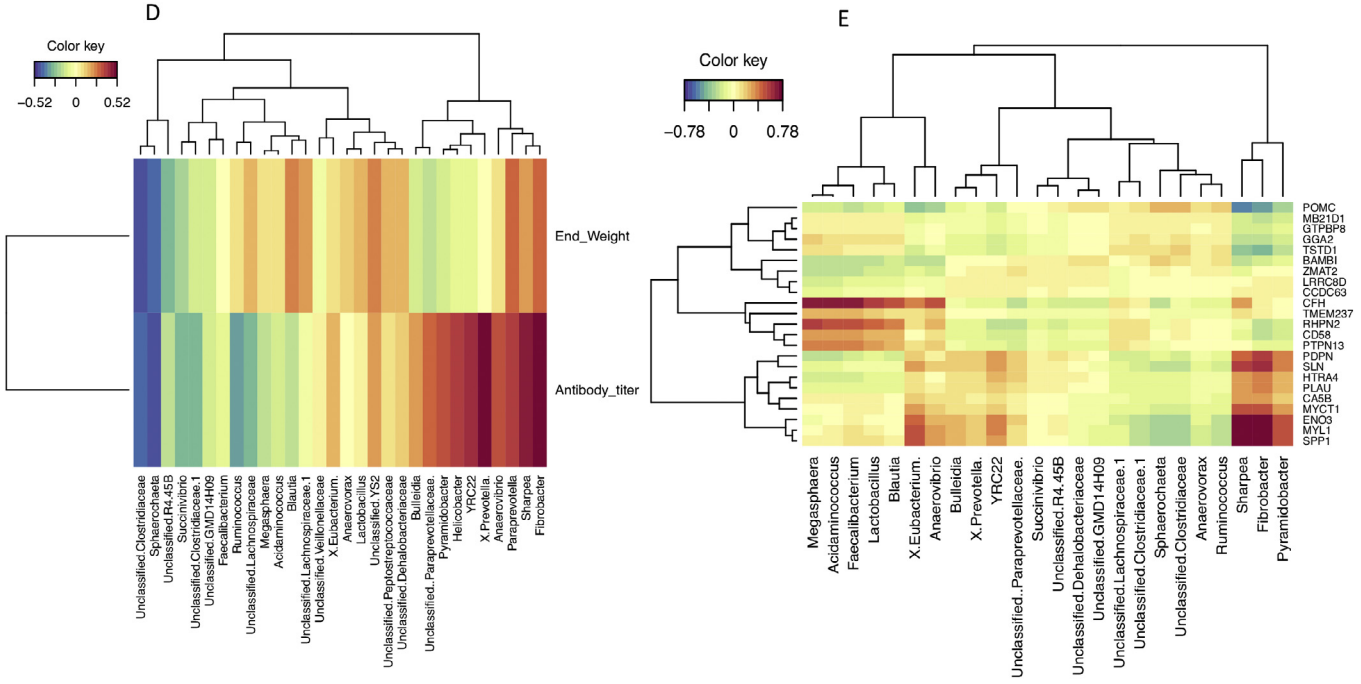

Fig. 5D-E. Correlation analysis at D0 time-point (at genus level). A; Clustered Image Map showing the correlation between the antibody titer and final body weight with the discriminant genera/taxa, B; Clustered Image Map showing the correlation between the selected genes with the discriminant genera/taxa. X. = means that the bacteria name should be in box brackets [].

plasminogen activator urokinase (*PLAU*), *complement 3* (*C3*), and *interleukin 1A* (*IL1A*) genes that partly contributed to the observed changes in biological functions, play significant roles in immune response, cell growth/proliferation and migration, cell–cell signalling, negative regulation of apoptosis, as well as regulation of the expression of interferon-gamma and interleukin-12 [44,45].

PLAU has also been implicated for the suppressor function of both human and murine regulatory T cells [46], whereas *SPP1* has been shown to increase at the injection site, 24 h following intramuscular injection with immunostimulating complex (ISCOM) vaccine combined with matrix adjuvant in pigs [47]. This may therefore explain their association with the observed immune cell activities; however, a direct link between these genes and vaccine response in pigs has not previously been reported.

The use of transcriptomics in identifying candidate gene biomarkers has been employed in cancer studies where the analysis of gene expression signatures of primary tumors [48,49] led to the identification of predictive outcome profiles [50,51]. Other strategies employed include the identification of predictive genes by empirical association with clinical symptoms, and then evaluation of those genes as potential biomarkers [52], or association of gene expression with selected immune traits coupled with additional validation studies [53]. We employed the empirical association of gene expression with antibody response, using a multivariate analysis, and discrimination approach in order to evaluate potential biomarkers. In this context, *SPP1*, *MYL1*, *HTRA4*, *ENO3*, *ADAM8*, *PROSER3*, *B4GALNT1*, and *MAP7D1*, were the most promising potential biomarkers as they also showed a correlation with the antibody titer, although there are no studies linking these genes to vaccine response in pigs. Also, *MYL1* was only expressed in few animals, a condition that excludes it from further considerations, and linear regression also revealed a poor association between the expression of the identified genes and the levels of antibody titers. Therefore, further validation studies will be required in order to ascertain the prediction potential of these candidate genes on the antibody response to *M. hyopneumoniae* vaccination in pigs. In humans, *HTRA4* is associated with altered gene expression and inflammation [54,55], and programmed cell death [56], whereas *ADAM8* has immunomodulation properties and is associated with the function of neutrophils during inflammatory responses [57].

Our second objective in the current study was to bring new insights in the potential contribution of early gut microbiota in the modulation of health and diseases in the context of vaccine response. More specifically we aimed to draw inferences about relationships between early dynamics of fecal microbiota as a potential predictor of vaccine response in pig husbandry. There is clear evidence that gut microbiota plays an important role in driving host metabolism and health [58,59]. Also, human and mouse studies have demonstrated the importance of commensal bacteria in immune responsiveness to infections in various ways, and to vaccines such as influenza, polio, and cholera toxins [5,11,13,60]. The studies also suggest that colonization by specific bacteria and minimized dysbiosis in early infancy may improve vaccine responses later in life, whereas other bacteria may lower vaccine response [61,62].

In this study, differences in vaccination response did not translate to changes in the composition and diversity of the microbial community, and bacterial diversity was also not predictive of vaccine response. However, OTUs belonging to Lachnospiraceae, *Parabacteroides distansosis*, *Bacteroides.* spp and *Sphaerochaeta* were more abundant in HR as early as PND7; although, only Lachnospiraceae and genera *Butyricimonas*, *Roseburia* and CF231, positively correlated with the antibody titer, and no further discernable correlations were evident at this time-point. At D0, OTUs belonging to *Prevotella.* Spp, *CF21*, Bacteroidales and S24-7 were more abundant in HR individuals, and correlation analysis revealed positive association between some of these OTUs (majorly *Prevotella*) with the antibody titer. Also, genera *Fibrobacter*, *Sharpea*, *Paraprevotella*, *Anaerovibrio*, [*Prevotella*], *YRC22*, *pyramidobacter*, and *Helicobacter* positively correlated with the antibody titer. We are unaware of studies evaluating the effects of these bacteria on *M. hyopneumoniae* vaccine response before or after vaccination in pigs. However, *Prevotella* is one of the most prevalent genera in the swine gastrointestinal tract, particularly after weaning, and besides their ability to degrade hemicelluloses in plant-based feed [63,64], a drastic decrease in their abundance in pigs has been associated with increased *Salmonella* shedding post-infection [65], suggesting extended health benefits. In pigs, it has also been reported that *Prevotella*-centered enterotypes are associated with a higher weight gain and production of luminal IgA [17,66], in line with positive influence of *Prevotella* on pig production and health. Also, in mice vaccinated with hepatitis B virus vaccine, LPS forms obtained from *Bacteroides* and *Prevotella* species were found to function *in vivo* as immunological adjuvants [67], and a *Prevotella* species, among others, was also found to positively correlate with influenza antibody titer levels at day 0 or post-vaccination time points, in a human study [60]. While the *Prevotella* species found in these studies may differ from the ones in our study, the results do support the potential of the members of this genus in promoting vaccine response. *Fibrobacter* spp. has been identified as an important cellulose-degrading bacteria with health benefits to the host [68], whereas Roseburia spp. are common gut bacteria that contribute to complex carbohydrate breakdown producing short chain fatty acids (SCFAs), particularity butyrate, which can affect colonic health [69], a similar role associated with *Butyricimonas* [70]. It is therefore not surprising that they were also positively associated with the final body weight.

Here, we also chose to integrate both the microbiota at D0 timepoint with the D2-selected genes, and we found positive correlations between expression of several genes (*MYL1*, *SPP1*, *ENO3*, *SLN*, and *PDPN*) and some OTUs (mainly OTUs belonging to *Prevotella*). However, this could be subjective since both the OTUs and the genes had already been selected and found to positively correlate with the antibody titers; therefore, caution should be exercised in interpreting these associations. Nevertheless, it may suggest a possible interaction between these OTUs and genes in promoting vaccine response, a condition that warrants future research. A major limitation of our study is the small sample size, which could have compromised the power to detect changes in expression between HR and LR pigs prior to or post-vaccination, and could also account for the minimal microbiota differences observed. Also, we are not certain whether the abundance of serum antibodies following vaccination translates to host protection. Further experiments are therefore required in order to further explore this topic, with more animals and in a disease challenge model.

In conclusion, although the current study failed to identify significant differences in expression of genes between HR and LR prior to *M. hyopneumoniae* vaccination that could potentially explain or predict vaccine response, empirical multivariate analysis and Ingenuity pathway analysis revealed differentially-modulated biological functions and broad processes of cellular movement and reorganization with respect to the phenotypic differences in antibody response to *M. hyopneumoniae*. Also, a few genes that correlated with the *M. hyopneumoniae*-specific antibodies 2 days post-vaccination, suggested a potential to predict vaccine response at early time-points post-vaccination, whereas differences in microbiota composition at the OTU level shows the potential of early-life microbiota in predicting vaccine response to *M. hyopneumoniae*, and informs a direction for future research.

Author contributions

B.P.W., G.P., J.W. conceived and designed the study/experiment; N.D., and J.W. performed the experiments; P.M.M, A.K., J.E., J.W., and J.F. analyzed the data; B.P.M., P.S., and G.P. provided

supervision of the project; P.M.M. wrote the paper. All authors reviewed and approved the final version of the manuscript.

Funding

The funding agencies had no role in the design of the study; in the collection, analyses, or interpretation of data; in the writing of the manuscript, and in the decision to publish the results.

Acknowledgement

The authors thank the University of Alberta Swine Research and Technology Centre, facility staff for their help with the animal trial (Animal care and monitoring, vaccination and sample collection). The authors also thank Yan Meng for her help with processing of blood samples. This work was financially supported by the Alberta Agriculture and Forestry project (2014F034R); and Genome Canada (2014 Genome Canada LSARP – Application of Genomics to Improve Disease Resilience and Sustainability in Pork Production). B.P.W. is supported by the Canada Research Chairs Program.

Conflict of interest

The authors declare no competing interests.

References

[1] Wilkie B, Mallard B. Selection for high immune response: an alternative approach to animal health maintenance? Vet Immunol Immunopathol 1999. https://doi.org/10.1016/S0165-2427(99)00136-1.
[2] Pasquale A, Preiss S, Silva F, Garçon N. Vaccine adjuvants: from 1920 to 2015 and beyond. Vaccines 2015. https://doi.org/10.3390/vaccines3020320.
[3] Andre FE, Booy R, Bock HL, Clemens J, Datta SK, John TJ, et al. Vaccination greatly reduces disease, disability, death and inequity worldwide. Bull World Health Organ 2008. https://doi.org/10.2471/BLT.07.040089.
[4] Henn AD, Wu S, Qiu X, Ruda M, Stover M, Yang H, et al. High-resolution temporal response patterns to influenza vaccine reveal a distinct human plasma cell gene signature. Sci Rep 2013. https://doi.org/10.1038/srep02327.
[5] Lynn DJ, Pulendran B. The potential of the microbiota to influence vaccine responses. J Leukoc Biol 2017. https://doi.org/10.1189/jlb.5MR0617-216R.
[6] Djordjevic SP, Eamens GJ, Romalis LF, Nicholls PJ, Taylor V, Chin J. Serum and mucosal antibody responses and protection in pigs vaccinated against Mycoplasma hyopneumoniae with vaccines containing a denatured membrane antigen pool and adjuvant. Aust Vet J 1997. https://doi.org/10.1111/j.1751-0813.1997.tb14383.x.
[7] Thacker EL, Thacker BJ, Boettcher TB. Jayappa H. Comparison of antibody production, lymphocyte stimulation, and protection induced by four commercial Mycoplasma hyopneumoniae bacterins. Swine Heal Prod 1998.
[8] Wesemann DR. Microbes and B cell development. Adv Immunol 2015. https://doi.org/10.1016/bs.ai.2014.09.005.
[9] Gensollen T, Iyer SS, Kasper DL, Blumberg RS. How colonization by microbiota in early life shapes the immune system. Science (80-) 2016. https://doi.org/10.1126/science.aad9378.
[10] Karst SM. The influence of commensal bacteria on infection with enteric viruses. Nat Rev Microbiol 2016. https://doi.org/10.1038/nrmicro.2015.25.
[11] Hall JA, Bouladoux N, Sun CM, Wohlfert EA, Blank RB, Zhu Q, et al. Commensal DNA limits regulatory T cell conversion and is a natural adjuvant of intestinal immune responses. Immunity 2008. https://doi.org/10.1016/j.immuni.2008.08.009.
[12] Eloe-Fadrosh EA, McArthur MA, Seekatz AM, Drabek EF, Rasko DA, Sztein MB, et al. Impact of oral typhoid vaccination on the human gut microbiota and correlations with S. Typhi-specific immunological responses. PLoS ONE 2013. https://doi.org/10.1371/journal.pone.0062026.
[13] Oh JZ, Ravindran R, Chassaing B, Carvalho FA, Maddur MS, Bower M, et al. TLR5-mediated sensing of gut microbiota is necessary for antibody responses to seasonal influenza vaccination. Immunity 2014. https://doi.org/10.1016/j.immuni.2014.08.009.
[14] Seekatz AM, Panda A, Rasko DA, Toapanta FR, Eloe-Fadrosh EA, Khan AQ, et al. Differential response of the cynomolgus macaque gut microbiota to shigella infection. PLoS ONE 2013. https://doi.org/10.1371/journal.pone.0064212.
[15] Yatsunenko T, Rey FE, Manary MJ, Trehan I, Dominguez-Bello MG, Contreras M, et al. Human gut microbiome viewed across age and geography. Nature 2012. https://doi.org/10.1038/nature11053.
[16] Zeng MY, Cisalpino D, Varadarajan S, Hellman J, Warren HS, Cascalho M, et al. Gut microbiota-induced immunoglobulin G controls systemic infection by symbiotic bacteria and pathogens. Immunity 2016. https://doi.org/10.1016/j.immuni.2016.02.006.
[17] Mach N, Berri M, Estellé J, Levenez F, Lemonnier G, Denis C, et al. Early-life establishment of the swine gut microbiome and impact on host phenotypes. Environ Microbiol Rep 2015. https://doi.org/10.1111/1758-2229.12285.
[18] Adler M, Murani E, Ponsuksili S, Wimmers K. PBMC transcription profiles of pigs with divergent humoral immune responses and lean growth performance. Int J Biol Sci 2013. https://doi.org/10.7150/ijbs.6769.
[19] Adler M, Murani E, Brunner R, Ponsuksili S, Wimmers K. Transcriptomic response of porcine PBMCs to vaccination with tetanus toxoid as a model antigen. PLoS ONE 2013. https://doi.org/10.1371/journal.pone.0058306.
[20] Adler M, Murani E, Ponsuksili S, Wimmers K. PBMC transcriptomic responses to primary and secondary vaccination differ due to divergent lean growth and antibody titers in a pig model. Physiol Genomics 2015. https://doi.org/10.1152/physiolgenomics.00015.2015.
[21] Gimsa U, Tuchscherer A, Gimsa J, Tuchscherer M. Assessing immune competence in pigs by immunization with tetanus toxoid. Animal 2018. https://doi.org/10.1017/S1751731117001197.
[22] Maes D, Segales J, Meyns T, Sibila M, Pieters M, Haesebrouck F. Control of Mycoplasma hyopneumoniae infections in pigs. Vet Microbiol 2008. https://doi.org/10.1016/j.vetmic.2007.09.008.
[23] Choi I, Hosseini A, Hua B, Kommadath A, Sun X, Meng Y, et al. Globin reduction in porcine whole blood for improving sensitivity and accuracy of transcriptome analysis. In: Proc int plant anim genome XXI 12-16 January 2013. CA USA San Diego; 2013. p. P0595.
[24] Kommadath A, Bao H, Arantes AS, Plastow GS, Tuggle CK, Bearson SMD, et al. Gene co-expression network analysis identifies porcine genes associated with variation in Salmonella shedding. BMC Genomics 2014. https://doi.org/10.1186/1471-2164-15-452.
[25] Groenen MAM, Archibald AL, Uenishi H, Tuggle CK, Takeuchi Y, Rothschild MF, et al. Analyses of pig genomes provide insight into porcine demography and evolution. Nature 2012. https://doi.org/10.1038/nature11622.
[26] Anders S, Pyl PT, Huber W. HTSeq – A Python framework to work with high-throughput sequencing data. Bioinformatics 2014. https://doi.org/10.1093/bioinformatics/btu638.
[27] Robinson MD, McCarthy DJ, Smyth GK. edgeR: a Bioconductor package for differential expression analysis of digital gene expression data. Bioinformatics 2010. https://doi.org/10.1093/bioinformatics/btp616.
[28] Lê Cao KA, Rossouw D, Robert-Granié C, Besse P. A sparse PLS for variable selection when integrating omics data. Stat Appl Genet Mol Biol 2008. https://doi.org/10.2202/1544-6115.1390.
[29] Lê Cao KA, Martin PGP, Robert-Granié C, Besse P. Sparse canonical methods for biological data integration: application to a cross-platform study. BMC Bioinf 2009. https://doi.org/10.1186/1471-2105-10-34.
[30] Rohart F, Gautier B, Singh A, Lê Cao K-A. mixOmics: an R package for 'omics feature selection and multiple data integration. PLOS Comput Biol 2017. https://doi.org/10.1371/journal.pcbi.1005752.
[31] Gonzalez I, Dejean S, Martin PGP, Baccini A. An R package to extend canonical correlation analysis. J Stat Softw 2008. https://doi.org/10.1359/JBMR.0301229.
[32] Conesa A, Nueda MJ, Ferrer A, Talón M. maSigPro: a method to identify significantly differential expression profiles in time-course microarray experiments. Bioinformatics 2006. https://doi.org/10.1093/bioinformatics/btl056.
[33] Willing BP, Vacharaksa A, Croxen M, Thanachayanont T, Finlay BB. Altering host resistance to infections through microbial transplantation. PLoS ONE 2011. https://doi.org/10.1371/journal.pone.0026988.
[34] Masella AP, Bartram AK, Truszkowski JM, Brown DG, Neufeld JD. PANDAseq: paired-end assembler for illumina sequences. BMC Bioinf 2012. https://doi.org/10.1186/1471-2105-13-31.
[35] Caporaso JG, Kuczynski J, Stombaugh J, Bittinger K, Bushman FD, Costello EK, et al. QIIME allows analysis of high-throughput community sequencing data. Nat Methods 2010. https://doi.org/10.1038/nmeth.f.303.
[36] Edgar R. UCHIME2: improved chimera prediction for amplicon sequencing. BioRxiv 2016. https://doi.org/10.1101/074252.
[37] Lozupone C, Knight R. UniFrac: a new phylogenetic method for comparing microbial communities. Appl Environ Microbiol 2005. https://doi.org/10.1128/AEM.71.12.8228-8235.2005.
[38] Vázquez-Baeza Y, Pirrung M, Gonzalez A, Knight R. EMPeror: a tool for visualizing high-throughput microbial community data. GigaScience 2013. https://doi.org/10.1186/2047-217X-2-16.
[39] Arumugam M, Raes J, Pelletier E, Le Paslier D, Yamada T, Mende DR, et al. Enterotypes of the human gut microbiome. Nature 2011. https://doi.org/10.1038/nature09944.
[40] Segata N, Izard J, Waldron L, Gevers D, Miropolsky L, Garrett WS, et al. Metagenomic biomarker discovery and explanation. Genome Biol 2011. https://doi.org/10.1186/gb-2011-12-6-r60.
[41] Knap P, Bishop S. Relationships between genetic change and infectious disease in domestic livestock. BSAP Occas Publ 2000;27:65–80.
[42] Regnström K, Ragnarsson EGE, Rydell N, Sjöholm I, Artursson P. Tetanus antigen modulates the gene expression profile of aluminum phosphate adjuvant in spleen lymphocytes in vivo. Pharmacogenomics J 2002. https://doi.org/10.1038/sj.tpj.6500080.
[43] Huang TH, Uthe JJ, Bearson SMD, Demirkale CY, Nettleton D, Knetter S, et al. Distinct peripheral blood RNA responses to Salmonella in pigs differing in Salmonella shedding levels: intersection of IFNG TLR and miRNA pathways. PLoS ONE 2011. https://doi.org/10.1371/journal.pone.0028768.

[44] Pennings JLA, Kimman TG, Janssen R. Identification of a common gene expression response in different lung inflammatory diseases in rodents and macaques. PLoS ONE 2008. https://doi.org/10.1371/journal.pone.0002596.
[45] Ropka-Molik K, Zukowski K, Eckert R, Gurgul A, Piõrkowska K, Oczkowicz M. Comprehensive analysis of the whole transcriptomes from two different pig breeds using RNA-Seq method. Anim Genet 2014. https://doi.org/10.1111/age.12184.
[46] He F, Chen H, Probst-Kepper M, Geffers R, Eifes S, Del Sol A, et al. PLAU inferred from a correlation network is critical for suppressor function of regulatory T cells. Mol Syst Biol 2012. https://doi.org/10.1038/msb.2012.56.
[47] Ahlberg V, Lövgren Bengtsson K, Wallgren P, Fossum C. Global transcriptional response to ISCOM-Matrix adjuvant at the site of administration and in the draining lymph node early after intramuscular injection in pigs. Dev Comp Immunol 2012. https://doi.org/10.1016/j.dci.2012.03.005.
[48] Ponomareva A, Rykova E, Cherdyntseva N, Skvortsova T, Dobrodeev A, Litviakov N, et al. Assay of methylated gene RARbeta2 in circulating DNA of blood from patients with lung cancer as a potential prognostic marker. Vopr Onkol 2011;57:302–7.
[49] Tóth K, Galamb O, Spisák S, Wichmann B, Sipos F, Leiszter K, et al. Free circulating DNA based colorectal cancer screening from peripheral blood: the possibility of the methylated septin 9 gene marker. Orv Hetil 2009. https://doi.org/10.1556/OH.2009.28625.
[50] Han M, Choong TL, Hong WZ, Chao S, Zheng R, Kok TY, et al. Novel blood-based, five-gene biomarker set for the detection of colorectal cancer. Clin Cancer Res 2008. https://doi.org/10.1158/1078-0432.CCR-07-1801.
[51] van Leeuwen DM, Gottschalk RWH, Schoeters G, van Larebeke NA, Nelen V, Baeyens WF, et al. Transcriptome analysis in peripheral blood of humans exposed to environmental carcinogens: a promising new biomarker in environmental health studies. Environ Health Perspect 2008. https://doi.org/10.1289/ehp.11401.
[52] Mohr S, Liew CC. The peripheral-blood transcriptome: new insights into disease and risk assessment. Trends Mol Med 2007. https://doi.org/10.1016/j.molmed.2007.08.003.
[53] Mach N, Gao Y, Lemonnier G, Lecardonnel J, Oswald IP, Estellé J, et al. The peripheral blood transcriptome reflects variations in immunity traits in swine: towards the identification of biomarkers. BMC Genomics 2013. https://doi.org/10.1186/1471-2164-14-894.
[54] Singh H, Zhao M, Chen Q, Wang Y, Li Y, Kaitu'U-Lino TJ, et al. Human HtrA4 expression is restricted to the placenta, is significantly Up-regulated in early-onset preeclampsia, and high levels of HtrA4 cause endothelial dysfunction. J Clin Endocrinol Metab 2015. https://doi.org/10.1210/jc.2014-3969.
[55] Wang Y, Nie G. High levels of HtrA4 observed in preeclamptic circulation drastically alter endothelial gene expression and induce inflammation in human umbilical vein endothelial cells. Placenta 2016. https://doi.org/10.1016/j.placenta.2016.09.003.
[56] Chien J, Campioni M, Shridhar V, Baldi A. HtrA serine proteases as potential therapeutic targets in cancer. Curr Cancer Drug Targets 2009. https://doi.org/10.2174/156800909788486704.
[57] Gomez-Gaviro M, Dominguez-Luis M, Canchado J, Calafat J, Janssen H, Lara-Pezzi E, et al. Expression and regulation of the metalloproteinase ADAM-8 during human neutrophil pathophysiological activation and its catalytic activity on L-selectin shedding. J Immunol 2007. https://doi.org/10.4049/jimmunol.178.12.8053.
[58] Isolauri E, Salminen S. The impact of early gut microbiota modulation on the risk of child disease: alert to accuracy in probiotic studies. Benef Microbes 2015. https://doi.org/10.3920/BM2014.0114.
[59] Rodríguez JM, Murphy K, Stanton C, Ross RP, Kober OI, Juge N, et al. The composition of the gut microbiota throughout life, with an emphasis on early life. Microb Ecol Heal Dis 2015. https://doi.org/10.3402/mehd.v26.26050.
[60] Salk HM, Simon WL, Lambert ND, Kennedy RB, Grill DE, Kabat BF, et al. Taxa of the nasal microbiome are associated with influenza-specific IgA response to live attenuated influenza vaccine. PLoS ONE 2016. https://doi.org/10.1371/journal.pone.0162803.
[61] Huda MN, Lewis Z, Kalanetra KM, Rashid M, Ahmad SM, Raqib R, et al. Stool microbiota and vaccine responses of infants. Pediatrics 2014. https://doi.org/10.1542/peds.2013-3937.
[62] Huda MN, Ahmad S, Kalanetra KM, Taft DH, Lewis ZT, Raqib R, et al. Infant stool microbiota at the time of vaccination at 6 w of age is associated with vaccine responses measured at 2 y of age. J Immunol 2017;198(139):1.
[63] Hayashi H, Shibata K, Sakamoto M, Tomita S, Benno Y. Prevotella copri sp. nov. and Prevotella stercorea sp. nov., isolated from human faeces. Int J Syst Evol Microbiol 2007. https://doi.org/10.1099/ijs.0.64778-0.
[64] Lamendella R, Santo Domingo JW, Ghosh S, Martinson J, Oerther DB. Comparative fecal metagenomics unveils unique functional capacity of the swine gut. BMC Microbiol 2011. https://doi.org/10.1186/1471-2180-11-103.
[65] Bearson SMD, Allen HK, Bearson BL, Looft T, Brunelle BW, Kich JD, et al. Profiling the gastrointestinal microbiota in response to Salmonella: low versus high Salmonella shedding in the natural porcine host. Infect Genet Evol 2013. https://doi.org/10.1016/j.meegid.2013.03.022.
[66] Ramayo-Caldas Y, Mach N, Lepage P, Levenez F, Denis C, Lemonnier G, et al. Phylogenetic network analysis applied to pig gut microbiota identifies an ecosystem structure linked with growth traits. ISME J 2016. https://doi.org/10.1038/ismej.2016.77.
[67] Chilton PM, Hadelq DM, To TT, Mitchell TC, Darveau RP. Adjuvant activity of naturally occurring monophosphoryl lipopolysaccharide preparations from mucosa-associated bacteria. Infect Immun 2013. https://doi.org/10.1128/IAI.01150-12.
[68] Ransom-Jones E, Jones DL, McCarthy AJ, McDonald JE. The fibrobacteres: an important phylum of cellulose-degrading bacteria. Microb Ecol 2012. https://doi.org/10.1007/s00248-011-9998-1.
[69] Flint HJ, Scott KP, Duncan SH, Louis P, Forano E. Microbial degradation of complex carbohydrates in the gut. Gut Microbes 2012. https://doi.org/10.4161/gmic.19897.
[70] Hamer HM, Jonkers D, Venema K, Vanhoutvin S, Troost FJ, Brummer RJ. Review article: the role of butyrate on colonic function. Aliment Pharmacol Ther 2008. https://doi.org/10.1111/j.1365-2036.2007.03562.x.